Electronic Supplementary Material (ESI) for New Journal of Chemistry

Exploring the Electrochemical Characteristics of the Nucleobase-Template Assisted $NiCo_2O_4$ Electrode Materials for Supercapacitors

Karthik Krishnan,[a*] Amuthan Dekshinamoorthy,[a] Saranyan Vijayaraghavan,[a] and Selvakumar Karuthapandi,[b*]
[a]Corrosion and Material Protection Division, CSIR-Central Electrochemical Research Institute, Karaikudi, Tamil Nadu-630003, India.
[b]Department of Chemistry, School of Advanced Sciences, VIT-AP University, Amaravati, Andhra Pradesh 522237, India.
*Corresponding author email: selvakumar.k@vitap.ac.in; karthikk@cecri.res.in

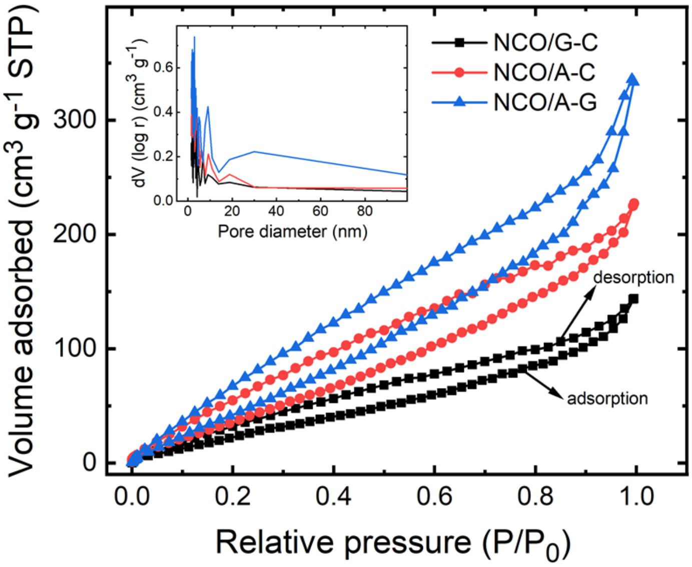

Figure S1. Nitrogen adsorption-desorption isotherms measured at 77 K for the NCO/G-C, NCO/A-C, and NCO/A-G nanostructures. The inset shows the corresponding Barrett–Joyner–Halenda (BJH) pore size distributions.

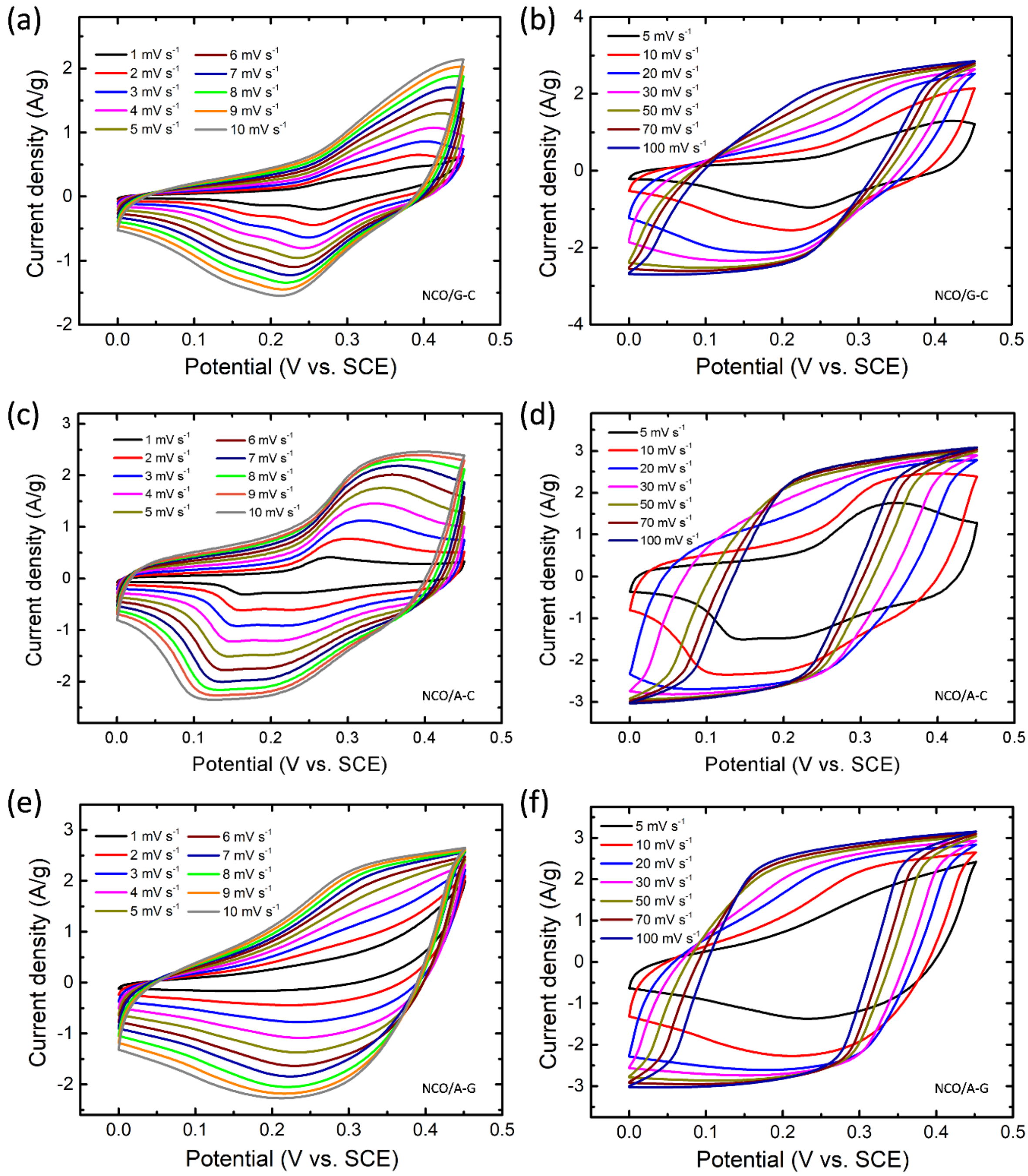

Figure S2. Typical cyclic voltammetry (CV) curves of the prepared NCO nanostructures using different combinations of nucleic acids such as (a, b) guanine (G)-cytosine (C), (c, d) adenine (A)-cytosine (C), and (e, f) adenine (A)-guanine (G), measured under various scan rates (1 mV s^{-1} to 100 mV s^{-1}) and a potential window of 0–4.5 V.

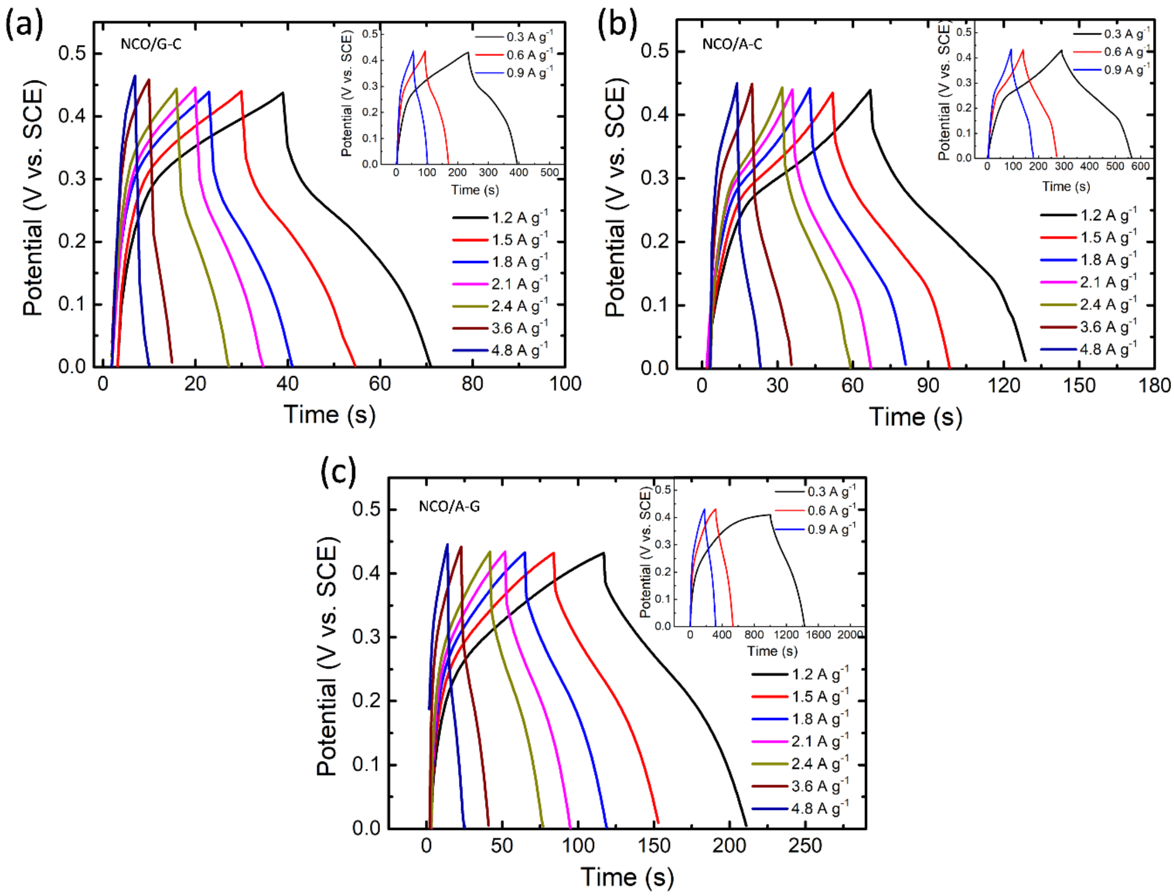

Figure S3. Typical galvanostatic charge–discharge (GCD) plots of the prepared NCO nanostructures using various combinations of nucleic acids such as (a) G-C (b) A-C and (c) A-G, measured under different current densities. The insets represent the lower current density ranges.

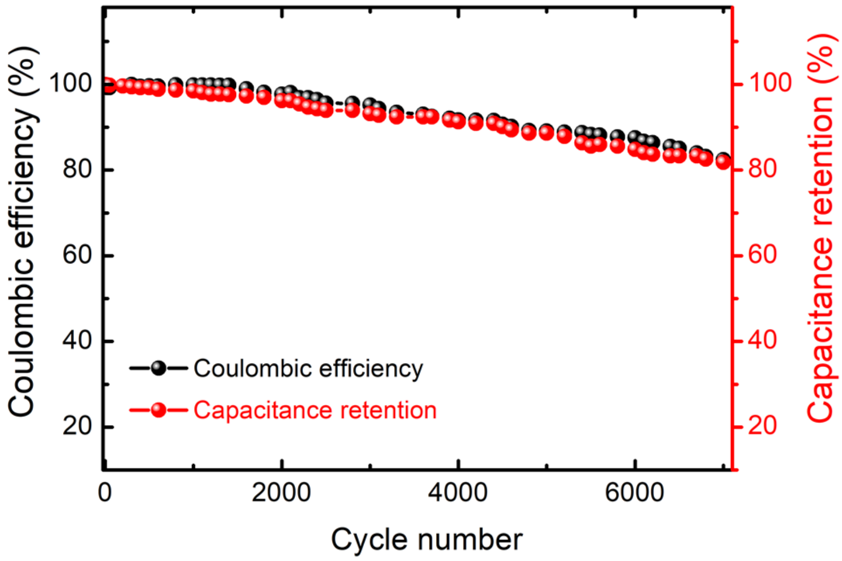

Figure S4. Capacitance retention characteristics of NCO/A-G nanostructures measured under 7000 continuous charge–discharge cycles at a constant current density of 3.6 A g^{-1} in a three-electrode configuration.

Table S1. Comparison of various electrochemical characteristics of NCO-based supercapacitor devices with the previously reported works.

Electrode Materials	**Electrolyte**	**Test condition**	**Specific capacity**	**Ref.**
$NiCo_2O_4$ nanoagglomerates	1M KOH	0.5 A g^{-1}	95.6 mA h g^{-1} (3-electrode)	[1]
honeycomb-structured $NiCo_2O_4$	2M KOH	0.5 A g^{-1}	140.1 mA h g^{-1}	[2]
3D rGO-PPy aerogels	2M KOH	0.5 A g^{-1}	72.2 mA h g^{-1}	[2]
$NiCo_2O_4$/Superactivated Carbon	2M KOH	1 A g^{-1}	24.6 mA h g^{-1}	[3]
Porous $NiCo_2O_4$ nanoplates	1M KOH	1 A g^{-1}	147 mA h g^{-1}	[4]
$NiCo_2O_4$ nanosheets	2M KOH	1 A g^{-1}	122.5 mA h g^{-1}	[5]
$NiCo_2O_4$ crystals	1M KOH	0.5 A g^{-1}	95.6 mA h g^{-1}	[6]
NCO/A-G (adenine-guanine)	3M KOH	0.3 A g^{-1}	130 mA h g^{-1}	This work

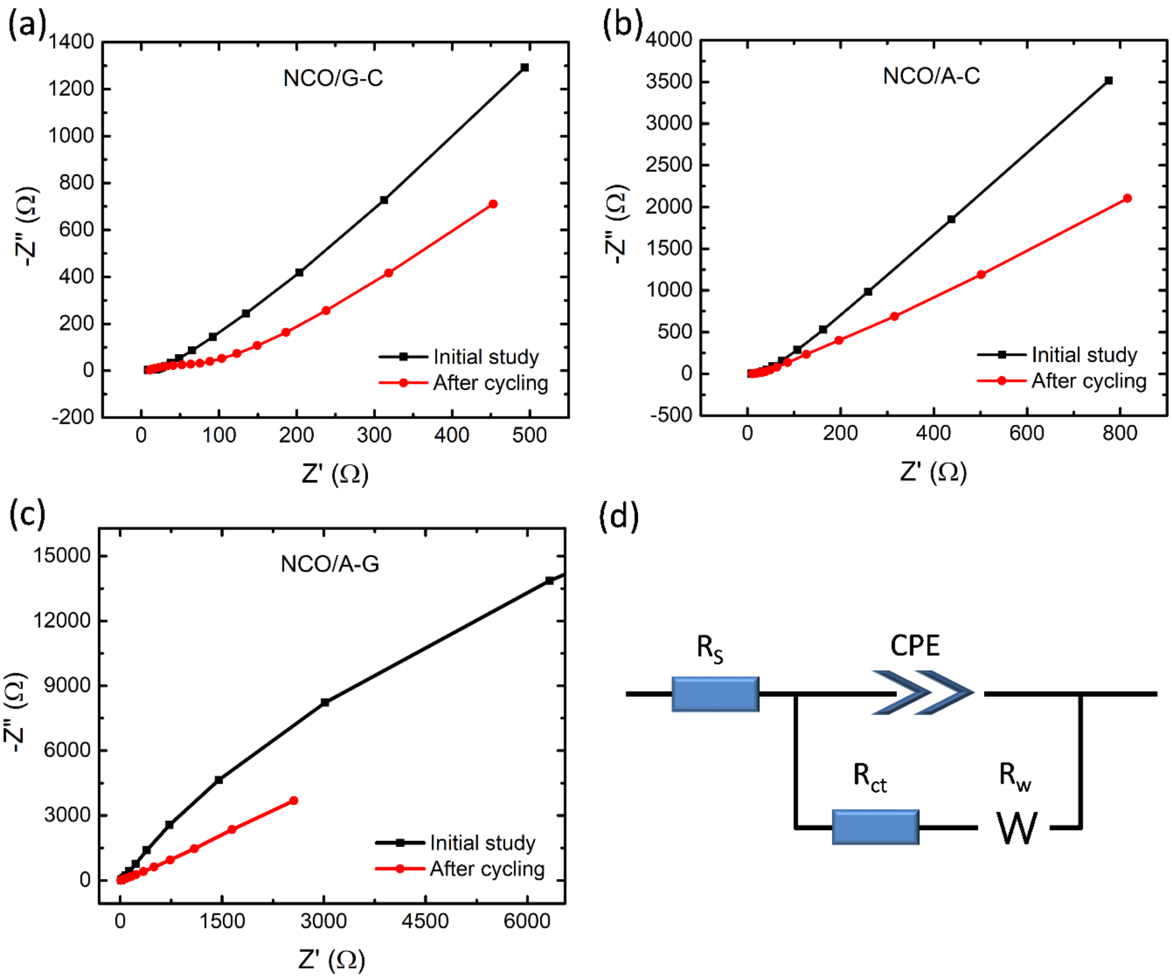

Figure S5. Nyquist plots of the prepared NCO nanostructures using various combinations of nucleic acids such as (a) G-C (b) A-C and (c) A-G, measured initially and after all the electrochemical characteristics. (d) The corresponding equivalent circuit model for the NCO-based supercapacitor device.

Table S2. The obtained electrical parameters of NCO-based supercapacitor devices from the EIS analysis

Devices	R_b (Ω cm^{-2})	R_{ct} (Ω cm^{-2})	R (Ω cm^{-2})	**Response at ϕ =45°**	
				Frequency (Hz)	**Time (s)**
NCO/G-C	18.9	51.8	89.1	11.22	$\tau_0 = 0.089$
NCO/A-C	15.6	28.8	33.9	28.78	$\tau_0 = 0.034$
NCO/A-G	12.3	10.1	22.1	122.86	$\tau_0 = 0.008$

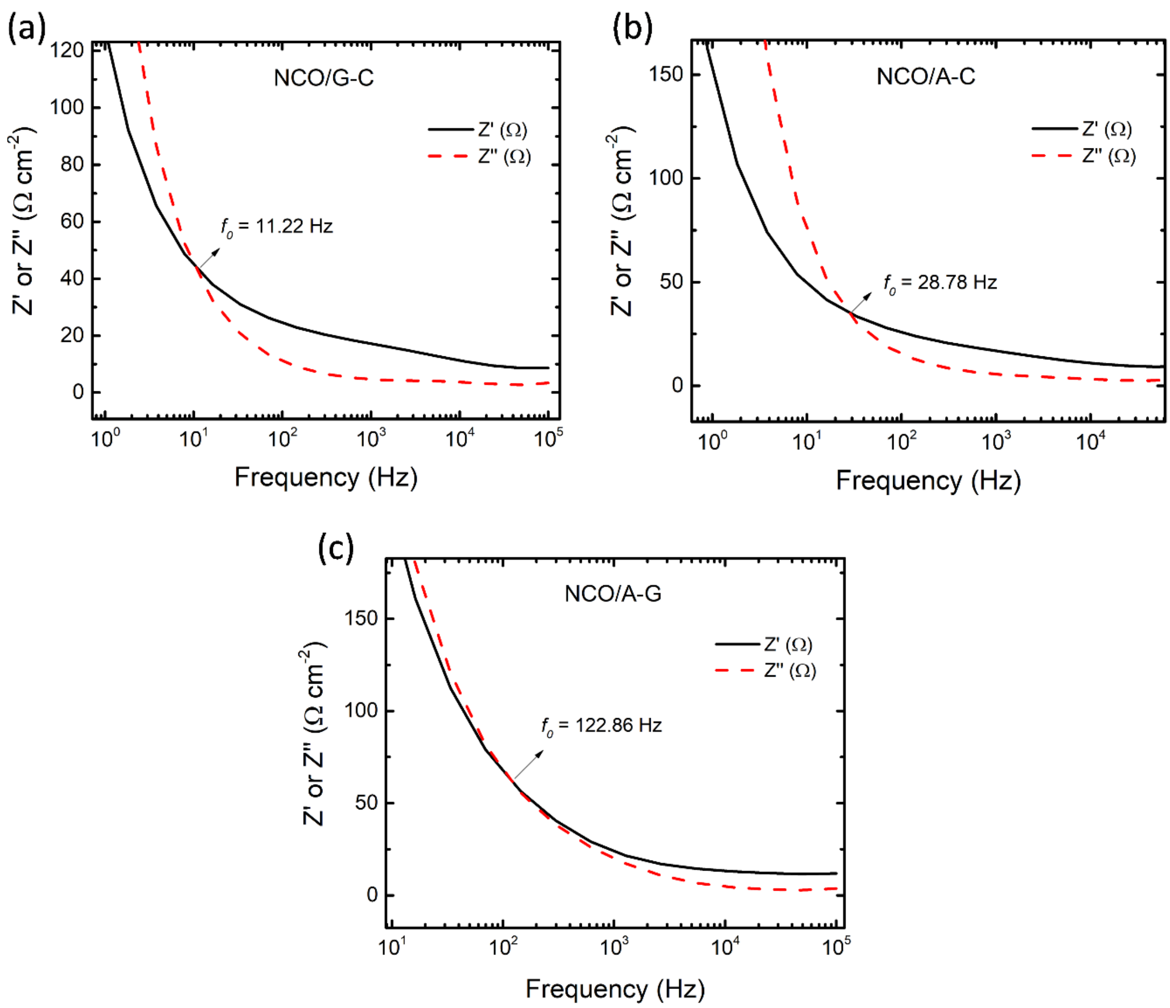

Figure S6 Bode's plots estimated from Millers approach using the EIS curves of (a) NCO/G-C, (b) NCO/A-C, and (c) NCO/A-G devices, respectively.

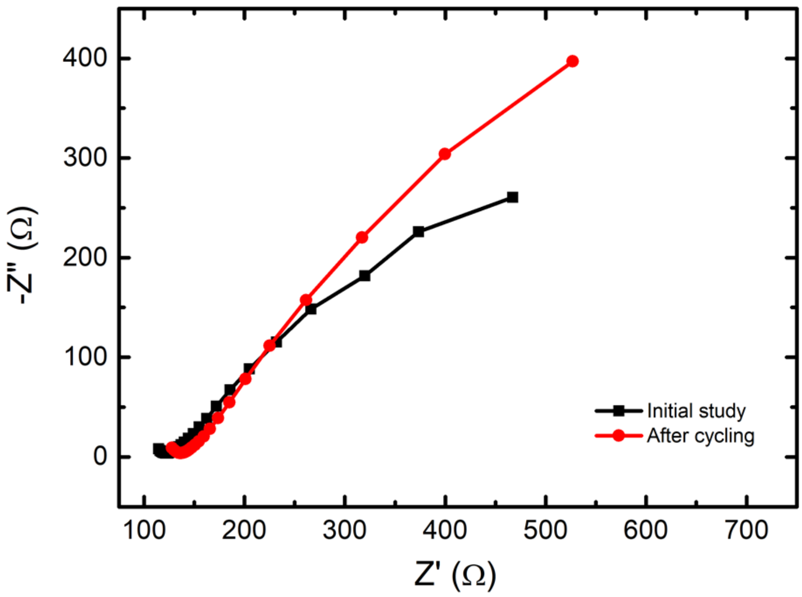

Figure S7. Nyquist plots of NCO/A-G based ASC device measured before and after all the electrochemical studies.

The GCD profiles of the six-serially assembled NCO/A-G-based ASC devices effectively light up a blue LED during discharging can be seen in the real-time movies **NCO-A-G ASC.mp4**.

References

1. K. O. Oyedotun, A. A. Mirghni, O. Fasakin, D. J. Tarimo, V. N. Kitenge, and N. Manyala, High-energy asymmetric supercapacitor based on the nickel cobalt oxide ($NiCo_2O_4$) nanostructure material and activated carbon derived from cocoa pods, *Energy & Fuels* 35, no. 24 (2021): 20309-20319.

2. C. Lai, X. Qu, H. Zhao, S. W. Hong, and K. Lee, Improved performance in asymmetric supercapacitors utilized by dual ion-buffering reservoirs based on honeycomb-structured $NiCo_2O_4$ and 3D rGO-PPy aerogels, *Applied Surface Science,* 586 (2022), 152847.

3. T. Panja, N. Díez, R. Mysyk, D. Bhattacharjya, E. Goikolea, and D. Carriazo, Robust $NiCo_2O_4$/Superactivated Carbon Aqueous Supercapacitor with High Power Density and Stable Cyclability, *ChemElectroChem*, 6 (9), (2019), 2536-2545.

4. J. Pu, J. Wang, X. Jin, F. Cui, E. Sheng, and Z. Wang, Porous hexagonal $NiCo_2O_4$ nanoplates as electrode materials for supercapacitor, *Electrochimica Acta* 106 (2013) 226-234.

5. H. Du, J. Lei, K. Xiang, W. Lin, J. Zheng, H. Liao, Facile synthesis of $NiCo_2O_4$ nanosheets with oxygen vacancies for aqueous zinc-ion supercapacitors, *J. Alloys Comp*. 896, (2022), 162925.

6. Y. Q. Wu, X. Y. Chen, P. T. Ji, and Q. Q. Zhou. "Sol–gel approach for controllable synthesis and electrochemical properties of $NiCo_2O_4$ crystals as electrode materials for application in supercapacitors." *Electrochimica Acta* 56, no. 22 (2011) 7517-7522.